

# Laser-Excited Atomic Fluorescence Spectrometry in a Pressure-Controlled Electrothermal Atomizer

Robert F. Lonardo, Alexander I. Yuzefovskiy,<sup>†</sup> Richard L. Irwin,<sup>‡</sup> and Robert G. Michel\*

Department of Chemistry, University of Connecticut, 215 Glenbrook Road, Storrs, Connecticut 06269-3060

**A theoretical model was developed to describe the loss of analyte atoms in graphite furnaces during atomization. The model was based on two functions, one that described the supply of analyte by vaporization, and another that described the removal of the analyte by diffusion. Variation in working pressure was shown to affect the competition between these two processes. Optimal atomization efficiency was predicted to occur at a pressure where the supply of the analyte was maximized, and gas phase interactions between the analyte and matrix were minimized. Experiments to test the model included the direct determination of phosphorus and tellurium in nickel alloys and of cobalt in glass. In all cases, reduction in working pressure from atmospheric pressure to 7 Pa decreased sensitivity by 2 orders of magnitude, but improved temporal peak shape. For the atomization of tellurium directly from a solid nickel alloy, and the atomization of cobalt from an aqueous solution, no change in sensitivity was observed as the working pressure was reduced from atmospheric pressure to ~70 kPa. If a reduction in working pressure affected only the diffusion of the analyte, poorer sensitivity should have been obtained. Only a commensurate increase in analyte vaporization could account for maintained sensitivity at lower working pressures. Overall, analyte vaporization was not dramatically improved at reduced working pressures, and maximum atomization efficiency was found to occur near atmospheric pressure.**

Atomic spectrometry in graphite furnaces, with an argon atmosphere, is well established for the determination of metals and metalloids in acid digests of samples and, to a lesser extent, for the direct determination of the elements in solid samples. For the analysis of solid materials, samples can be introduced directly into the furnace or presented as a slurry. Bendicho and de Loos-Vollebregt<sup>1</sup> reviewed the literature of the solid sampling technique and compiled a comprehensive table that depicted analytes sought, sample matrices, atomizers, and analytical precision and accuracy. Modern graphite furnace techniques are based upon stabilized temperature platform furnace (STPF) technology.<sup>2,3</sup> The essence of STPF technology is complete atomization of the analyte with a

minimum of chemical and physical interferences. Some of the conditions required for complete atomization are chemical modification of the matrix, high heating rate, pyrolytically coated graphite furnaces, and use of the L'vov platform.<sup>3</sup> The usefulness of atomization at pressures other than atmospheric pressure has not been extensively explored. This paper reports research that had three objectives. The first was to investigate whether or not involatile elements could be vaporized more easily to give higher sensitivity at pressures lower than at 1 atm. The second was to explore literature reports that matrix interferences of graphite furnace atomic spectrometry might be minimized by vaporization at reduced pressures. The third was to determine whether or not a decrease in the working pressure might improve the direct analysis of solid samples through increased atomization efficiency.

In electrothermal atomizer atomic absorption spectrophotometry (ETA-AAS), pressure regulation has been investigated<sup>4–10</sup> as a means to improve the vaporization of involatile elements, increase the linear dynamic range, and eliminate matrix effects associated with the direct analysis of solid samples. L'vov<sup>4,5</sup> and Sturgeon et al.<sup>6</sup> showed that increased pressure lengthened the residence time of the analyte vapor inside the furnace and resulted in a broadened absorption spectral line profile, decreased sensitivity, and shifted linear dynamic range. Donega and Burgess<sup>7</sup> investigated the effect of foreign gas pressure on the absorption signals of aluminum and sodium in vacuum electrothermal atomizer atomic absorption spectrometry (VETA-AAS) with graphite boat atomization. The absorbance signals were found to increase as the working pressure was increased from 0.13 to 13 kPa and remain relatively constant as the pressure was increased further to 40 kPa. No data were reported for pressures above 40 kPa. The increase in sensitivity at pressures lower than 1 atm was postulated to be the result of a reduction in foreign gas effects. Wang and Holcombe<sup>8</sup> examined the sensitivity and linear dynamic range of VETA-AAS with STPF technology for cadmium, copper, manganese, and vanadium. Low-pressure atomization decreased sensitivity and shifted the linear dynamic ranges from the low nanogram per milliliter region to the high milligram per milliliter region. Hassell et al.<sup>9</sup> investigated VETA-AAS with STPF technology for lead and vanadium. They observed a reduction in

<sup>†</sup> Present address: Research Center, Philip Morris U.S.A., Richmond, VA 23234.

<sup>‡</sup> Present address: Pfizer Inc., Groton, CT 06340.

(1) Bendicho, C.; de Loos-Vollebregt, M. T. C. *J. Anal. At. Spectrom.* **1991**, *6*, 353–374.

(2) *Analytical Methods for Atomic Spectroscopy*; Perkin-Elmer Corp., Norwalk, CT, 1982.

(3) Slavin, W. *Graphite Furnace AAS: A Source Book*; Perkin-Elmer Corp., Ridgefield, CT, 1984.

(4) L'vov, B. V. *Atomic Absorption Spectrochemical Analysis*, 2nd ed.; Hilger: London, 1970.

(5) L'vov, B. V. *Spectrochim. Acta, Part B* **1978**, *33B*, 153–193.

(6) Sturgeon, R. E.; Chakrabarti, C. L.; Bertels, P. C. *Spectrochim. Acta, Part B* **1977**, *32B*, 257–277.

(7) Donega, H. M.; Burgess, T. E. *Anal. Chem.* **1970**, *42*, 1521–1524.

(8) Wang, P.; Holcombe, J. A. *Spectrochim. Acta, Part B* **1992**, *47B*, 1277–1286.

(9) Hassell, D. C.; Rettberg, T. M.; Fort, F. A.; Holcombe, J. A. *Anal. Chem.* **1988**, *60*, 2680–2683.

(10) Bekov, G. I.; Kurshii, A. N.; Letokhov, V. S.; Radaev, V. N. *Zh. Anal. Chim.* **1985**, *40*, 2208–2215.

sensitivity by 2 orders of magnitude, and narrower temporal signal profiles, as the working pressure was reduced from 1 atm to 20 Pa. Hassell et al.<sup>9</sup> determined lead in phosphorized copper, Standard Reference Material (SRM) 1253a, by VETA-AAS with STPF technology. Quantitative analyses were in excellent agreement with certified values, owing to complete atomization of lead from the less volatile solid copper matrix, with minimum matrix interference. Furthermore, the appearance of multiple peaks in the signal profiles represented the possibility of differentiation between the various forms and/or locations of lead in the solid sample. Low-pressure vaporization has also been applied to remove matrix interferences associated with the analysis of solid samples. Bekov and co-workers<sup>10</sup> employed vacuum laser photoionization spectroscopy for the determination of trace amounts of ruthenium in geological samples (GSO No. 935-76) that consisted primarily of copper. The relatively volatile copper matrix was removed by use of a char step at reduced pressure, after which complete ruthenium atomization was achieved.

The use of low-pressure vaporization to remove matrix interferences associated with the analysis of solid samples has been coupled with electrothermal atomizer laser-excited atomic fluorescence spectrometry (ETA-LEAFS).<sup>11–13</sup> ETA-LEAFS has been demonstrated to have femtogram detection limits, linear dynamic ranges of 5–7 orders of magnitude, freedom from spectral interferences, and low matrix effects.<sup>14–17</sup> Bolshov et al.<sup>11–13</sup> employed vacuum electrothermal atomizer laser-excited atomic fluorescence (VETA-LEAFS) without STPF technology for the determination of cobalt in silicon dioxide, quartz glass, tin, and plants and for the determination of ruthenium in lead and copper alloys. For all analyses, a char step was conducted under vacuum that removed the matrix without loss of analyte. As a result, matrix effects were eliminated, and quantitative results for real sample analyses were in agreement with certified values. Low-pressure vaporization was found to degrade the detection limits by 2 orders of magnitude. However, similar solid sample analyses conducted at atmospheric pressure were unsuccessful due to an inability to remove the sample matrices prior to atomization of the analyte. Intense laser scatter off the residual sample matrices prevented accurate quantitative analyses.

Bolshov et al.<sup>11,12,13</sup> did not employ STPF technology, which led us to hypothesize that VETA-LEAFS combined with STPF technology might improve the determination of involatile elements, in either solution or solid samples. In the current research, we studied a variety of analytes in different matrices in order to test this hypothesis. Previously in our laboratory, solid sampling by ETA-LEAFS at atmospheric pressure was used for the determination of phosphorus<sup>16</sup> and tellurium<sup>17</sup> in different types of high-temperature nickel-based alloys. Quantitative analysis was possible for tellurium, but not phosphorus, due to its involatility in the nickel matrices. In the current work, we attempted to improve

the atomization efficiency by a reduction in working pressure. Finally, a preliminary study was conducted for the determination of platinum by VETA-LEAFS. This element was chosen not only for its involatility but also for its convenient accessibility to our instrumentation at the time.

## THEORY

Several investigations have been made to understand how a reduction in working pressure affects analyte atomization. Recently, Chekalin et al.<sup>18</sup> used VETA-LEAFS to study the mechanisms associated with analyte atomization. General models that describe the loss of atoms in graphite furnaces have been proposed by L'vov,<sup>5</sup> van den Broek and de Galan,<sup>19</sup> and Falk and Schnürer.<sup>20</sup> According to these models, the maximum number of analyte atoms inside the atomizer during atomization ( $N_{\max}$ ) can be expressed as

$$N_{\max} = \eta(\tau_1/\tau_2)N_0 \quad (1)$$

where  $N_0$  is the total number of analyte atoms introduced into the atomizer;  $\tau_1$  is the supply function, which is the average time required for the analyte atoms to be transferred into the gaseous phase during the atomization cycle;  $\tau_2$  is the removal function, which is the average residence time of the analyte atoms in the gaseous phase; and  $\eta$  is a correction factor that depends on the ratio of  $\tau_1/\tau_2$  and the vaporization mode. The vaporization mode is characteristic of the heating rate of the atomizer and any chemical or physical reactions undergone by the analyte during atomization. This model is a relatively simple approximation based on the assumption that there is complete sample atomization, a homogeneous distribution of atoms across the tube cross section, no dosing hole, a constant temperature along the furnace, a constant concentration gradient of atoms along the furnace from the center to the edges, a negligibly small loss of analyte atoms due to diffusion during the atomization time,<sup>20</sup> and the probe zone fills the bore of the furnace. Furthermore,  $\tau_2$  has been shown to be related to the diffusion coefficient ( $D$ )<sup>20</sup> by

$$\tau_2 = l^2/8D \quad (2)$$

and

$$D = D_0[p_0/p][T/T_0]^n \quad (3)$$

where  $l$ ,  $p$ , and  $T$  are the length of the atomizer, working pressure, and atomization temperature, respectively.  $D_0$ ,  $p_0$ ,  $T_0$  represent standard conditions, and  $1.5 < n < 2$ .

The integral value of  $N_{\max}$  is the peak area ( $Q_a$ ), and for a constant atomization temperature,  $N_{\max}$  decreases as the pressure increases, while  $Q_a$  remains constant. This is true when  $\tau_2 \gg \tau_1$ , Lorentz broadening prevails over Doppler broadening, and the absorbance is measured at the maximum of the unshifted absorption profile. Thus, there exists a pressure range where  $N_{\max}$  is inversely proportional to pressure while both  $Q_a$  and  $T$  are

(11) Bolshov, M. A.; Zybin, A. V.; Koloshnikov, V. G.; Smirenkina, I. I. *Spectrochim. Acta, Part B* **1988**, *43B*, 519–528.

(12) Bolshov, M. A.; Zybin, A. V.; Koloshnikov, V. G.; Mayorov, I. A.; Smirenkina, I. I. *Spectrochim. Acta, Part B* **1986**, *41B*, 487–492.

(13) Bolshov, M. A.; Zybin, A. V.; Koloshnikov, V. G.; Smirenkina, I. I. *Ind. Lab. (Engl. Transl.)* **1989**, *55*, 1028–1034.

(14) Butcher, D. J.; Dougherty, J. P.; Preli, F. R.; Walton, A. P.; Wei, G.-T.; Irwin, R. L.; Michel, R. G. *J. Anal. At. Spectrom.* **1988**, *3*, 1059–1078.

(15) Sjöström, S. *Spectrochim. Acta Rev.* **1990**, *13*, 407.

(16) Liang, Z.; Lonardo, R. F.; Takahashi, J.; Michel, R. G. *J. Anal. At. Spectrom.* **1992**, *7*, 1019–1028.

(17) Liang, Z.; Lonardo, R. F.; Michel, R. G. *Spectrochim. Acta, Part B* **1993**, *48B*, 7–23.

(18) Chekalin, N.; Marunkov, A.; Axner, O. *Spectrochim. Acta, Part B* **1994**, *49B*, 1411–1435.

(19) van den Broek, W. M. G. T.; de Galan, L. *Anal. Chem.* **1977**, *49*, 2176–2186.

(20) Falk, H.; Schnürer, C. *Spectrochim. Acta, Part B* **1989**, *44B*, 759–770.

constant. For the opposite situation, where the pressure is decreased inside the atomizer, an increase in diffusion results in a decrease in  $\tau_2$  and an ultimate decrease in  $N_{\max}$  and  $Q_a$ . These results were experimentally confirmed by Hassell et al.<sup>9</sup>

**Effect of Low-Pressure Vaporization on Analytical Sensitivity in Graphite Furnaces.** A model that can express  $N_{\max}$  as a function of pressure is required in order to predict optimum atomization conditions for different analytes. From the above discussion, there should be some pressure that corresponds to a maximum  $N_{\max}$  at a constant atomization temperature. At this pressure,  $N_{\max}$  should depend only on the volatility of the analyte, the diffusion rate for the given atomizer, and the volume of the probe zone. In order to develop a relationship for  $N_{\max}$  as a function of pressure, we need to consider how  $Q_a$  will be affected under atomization control and under diffusion control. Atomization control refers to analyte atomization in a low-pressure environment, where  $\tau_2 \gg \tau_1$  and  $Q_a$  depends primarily on the atomization rate. Diffusion control corresponds to vaporization at higher pressures where  $\tau_2 \rightarrow \tau_1$  and  $Q_a$  depends primarily on the rate at which the analyte diffuses out of the atomizer during atomization. To a first approximation, we can assume that each analyte atom in the furnace does not absorb any laser radiation during the time required for vaporization and only absorbs energy during its residence time in the probe zone. Therefore, the total time ( $\tau_t$ ) that each atom spends on atomization and diffusion during the atomization cycle is

$$\tau_t = \tau_1 + \tau_2 \quad (4)$$

Under atomization control where  $\tau_2 \gg \tau_1$ ,  $\tau_t \approx \tau_2$ , and

$$Q_a = N_0 \tau_2 = N_0 (\tau_t - \tau_1) \approx N_0 (\tau_2 - \tau_1) \quad (5)$$

The difference  $(\tau_t - \tau_1) \approx (\tau_2 - \tau_1)$  can be interpreted as the absolute time that each analyte atom is available for excitation. In order to use this model quantitatively, the relative fraction of time ( $\alpha$ ) that each atom spends in the gaseous phase and the integrated signal for any given diffusion rate ( $Q_a$ ) are required. Since  $\alpha$  is defined as the ratio of  $\tau_2$  to  $\tau_1$  and  $\tau_2 \gg \tau_1$ ,

$$\alpha = \frac{\tau_t - \tau_1}{\tau_t} \approx \frac{\tau_2 - \tau_1}{\tau_2} \quad (6)$$

Substitution into eq 5 yields

$$Q_a \approx N_0 (\tau_2 - \tau_1) = N_0 \tau_2 \frac{(\tau_2 - \tau_1)}{\tau_2} = N_0 \tau_2 \alpha \rightarrow Q_a = Q_a \alpha \quad (7)$$

In the case of atomization control, the analyte will diffuse out of the atomizer more slowly than it will appear in the gaseous phase, thus  $\alpha \rightarrow 1$  and  $Q_a$  will remain constant for different atomization conditions. The value will depend primarily on  $N_0$  and  $\tau_2$ . In the case of diffusion control,  $\tau_2 \rightarrow \tau_1$ ,  $\alpha \rightarrow 0$ , and  $Q_a$  will decrease. Figure 1 is a graphical representation of diffusion and atomization control. In Figure 1a, the relative fraction of time available for analyte excitation,  $\alpha$ , was plotted as a function of  $\tau_2/\tau_1$ . In order to simplify the calculations,  $\tau_1$  was assumed to be unity, and  $\tau_2$  was increased by 3 orders of magnitude with respect

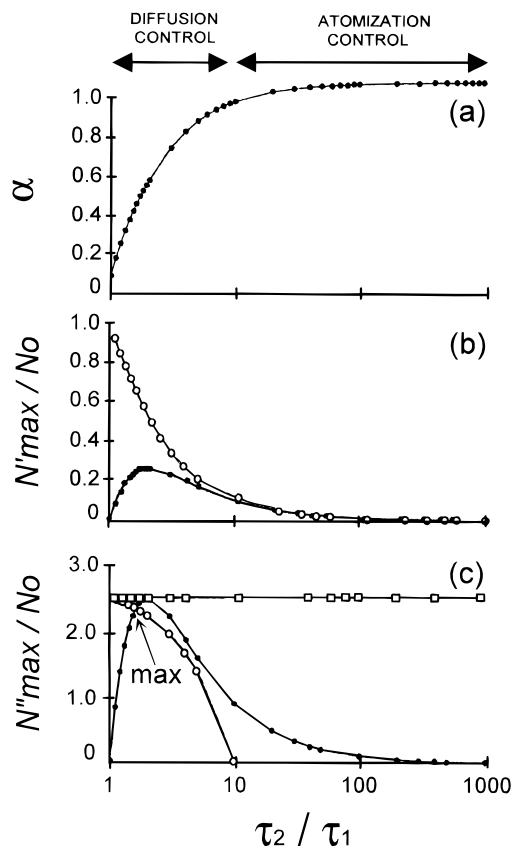


Figure 1. (a) Fraction of atom available for excitation as a function of removal and supply functions. (b) Relative maximum number of atoms in a peak profile: (○) L'vov's model<sup>4</sup> and (●) our model for  $N'_{\max}$ . (c) Relative maximum number of atoms in a peak profile: (●) our model for  $N_{\max}$  without chemical interference, (□) our model for  $N'_{\max}$  without chemical interference,  $\Omega = 0$ ; and (○) our model for  $N'_{\max}$  with chemical interference,  $\Omega = 0.11$ .

to  $\tau_1$ . As  $\tau_2/\tau_1$  is increased from 1 to 10,  $\alpha$  is increased from 0 to 0.9. The region where  $\alpha$  is proportional to  $\tau_2/\tau_1$  is the diffusion control region. As  $\tau_2/\tau_1$  is increased further,  $\alpha$  does not change significantly, and this region can be associated with atomization control. For example, when  $\tau_2/\tau_1 = 10$ ,  $\alpha = 0.9$ , and eq 7 transforms into eq 5 with a relative error of 10%. Therefore, the losses of the analytical signal  $Q_a$  due to diffusion from the atomizer should not exceed 10% in the atomization control region, for the purpose of this theory.

In the case of diffusion control,  $N_{\max}$  can be described in a fashion similar to  $Q_a$ . As  $Q_a$  is not constant,  $N_{\max}$  decreases simultaneously with  $Q_a$  and can be expressed as

$$N_{\max} = \delta Q_a / \delta t \quad (8)$$

The peak number of atoms available for excitation at a given diffusion rate,  $N_{\max}$ , is proportional to  $Q_a$ ; therefore,

$$\frac{Q_a}{Q_a} \approx \frac{N_{\max}}{N_{\max}} = \alpha \quad (9)$$

Substitution into eqs 1 and 9 yields

$$N_{\max} = \alpha N_{\max} = \alpha \eta \left( \frac{\tau_1}{\tau_2} \right) N_0 = \left( 1 - \frac{\tau_1}{\tau_2} \right) \eta \left( \frac{\tau_1}{\tau_2} \right) N_0 = w \eta N_0 \quad (10)$$

where  $w = (\tau_1/\tau_2) (1 - \tau_1/\tau_2)$ . Thus,  $N_{\max} \sim w$  for a constant  $N_0$ .

The dependence of  $N_{\max}/N_0$  on  $\tau_2/\tau_1$  is shown in Figure 1b for both our model and L'vov's<sup>5</sup> model with the assumption that  $\eta = \tau_1 = 1$ . In the atomization control region where  $\tau_2/\tau_1 \geq 10$ , our model approaches L'vov's model. However, in the diffusion-controlled region where  $\tau_2 \rightarrow \tau_1$ , our model shows that  $N_{\max}/N_0$  reaches a maximum and then decreases, while  $N_{\max}/N_0$  increases asymptotically in L'vov's model. L'vov's<sup>5</sup> model did not include losses of the absorbance signal due to an increased diffusion rate and is not useful in the diffusion-controlled region. In the present model, the optimum condition for analyte atomization occurs at the largest  $N_{\max}/N_0$  ratio that corresponds to the best signal-to-noise ratio. The derivative of  $\tau_2/\tau_1$  with respect to  $N_{\max}/N_0$  in eq 10 shows this situation to occur when the removal function ( $\tau_2$ ) is 2 times larger than the supply function ( $\tau_1$ ). Due to the general nature of  $\tau_2/\tau_1$ , this model is valid for all analytes of the same volatility, but not for samples with complex matrices where some chemical interactions may be involved. Although the model does not have the ability to predict an optimum atomization pressure or temperature from fundamental parameters only, an understanding of the shift in the atomization efficiency as a function of pressure is provided.

**Proposed Role of Chemical Interferences.** Probably the most common example of a chemical interference is the effect of a second element that chemically interacts with the analyte during atomization to form a stable molecule in the gas phase. Such a chemical interference would decrease  $Q_a$  and ultimately decrease  $N_{\max}$ . A significant decrease in  $N_{\max}$  can degrade the analyte sensitivity and, thus, the detection limit. Here, the above model is used to predict the optimum conditions for the atomization of analyte A in the presence of a chemical interference B. The model is based on several assumptions. First, all analyte losses are due to the formation of stable A–B dimers. Second, both A and B types of atoms are present in the gaseous phase simultaneously. And third, all interactions occur only during  $\tau_2$ . Hence, the total number of interactions of analyte atoms during  $\tau_2$  can be expressed as

$$Z_{\text{tot}} = Z_{A-B} + Z_{A-A} + Z_{A-G} + Z_{A-W} \quad (11)$$

where  $Z_{A-B}$ ,  $Z_{A-A}$ ,  $Z_{A-G}$ , and  $Z_{A-W}$  are the number of collisions between A and B atoms, A atoms, A and foreign gas atoms G, and A atoms and the wall of the atomizer W, respectively. In real situations,  $Z_{A-A}$  and  $Z_{A-W}$  can result in losses of analyte by the formation of dimers and trapping effects between the analyte and wall of the furnace, respectively. The goal of this section is to consider losses of analyte due only to the presence of a single chemical interference. Thus, analyte losses are assumed to result only from  $Z_{A-B}$  interactions, while all other types of collisions are assumed to affect only the residence time of the analyte. The kinetic theory of gases gives the collision frequency between A and B atoms per unit volume per unit time<sup>21</sup> as

$$Z_{A-B} = \pi d^2 (8kT/\pi\mu)^{1/2} (N_A N_B / V^2) \quad (12)$$

where  $d$ ,  $k$ ,  $T$ ,  $\mu$ ,  $N_A$ ,  $N_B$ , and  $V$  represent the reduced diameter, Boltzmann constant, temperature, reduced mass, number of

analyte atoms in the probe volume, number of matrix atoms in the probe volume, and probe volume, respectively. For simplicity, the probe volume is assumed to be unity. The total number of collisions per unit volume between A and B atoms in the probe volume during  $\tau_2$  is

$$Z_{A-B} = z_{A-B} \tau_2 \quad (13)$$

and the total number of molecules per unit volume that form as a result of these collisions is

$$N_{A-B} = \psi Z_{A-B} = \psi z_{A-B} \tau_2 \quad (14)$$

where the fraction of effective collisions,  $\psi$ , is a value between 0 and 1 and constant for particular A and B atoms. Substitution of eq 12 into 14 yields

$$N_{A-B} = \psi \pi d^2 (8kT/\pi\mu)^{1/2} (N_A N_B / V^2) \tau_2 = \psi C N_A N_B \tau_2 \quad (15)$$

where  $C = \pi d^2 (8kT/\pi\mu)^{1/2} / V^2$  and is a constant for a given temperature, probe volume, and chemical species. With the assumption that all analyte losses are due to the formation of stable A–B dimers, the total number of free atoms available for excitation in the gas phase,  $N_0$ , will be reduced by  $\psi C N_A N_B \tau_2$ . The reduced number of free atoms available for excitation in the gas phase,  $N_o$ , can be expressed as

$$N_o = N_A - N_{A-B} = N_A (1 - \psi C N_B \tau_2) \quad (16)$$

where  $0 \leq N_{A-B} \leq N_0$  and  $0 \leq \psi C N_B \tau_2 \leq 1$ . Similarly, the maximum number of atoms in the peak in the presence of a matrix interference,  $N'_{\max}$ , can be represented as

$$N'_{\max} = N_A (1 - \psi C N_B \tau_2) = N_{\max} (1 - \Omega \tau_2) \quad (17)$$

where  $\Omega = \psi C N_B$  and is a constant between 0 and 1.

Figure 1c shows graphical solutions of  $N'_{\max}/N_0$  as a function of  $\tau_2/\tau_1$ , for  $\Omega = 0$  and  $\Omega = 0.11$ , which represent the absence and presence of matrix interferences, respectively. The plot of  $N_{\max}/N_0$  versus  $\tau_2/\tau_1$ , presented in Figure 1b, is shown for comparison. In the absence of a chemical interference,  $N'_{\max} = N_{\max}$  and remains constant for all pressures. The plot for  $\Omega = 0$  is not identical to the plot of  $N_{\max}/N_0$  versus  $\tau_2/\tau_1$  (filled circles) because the model for  $N'_{\max}$  assumes  $\tau_1$  is constant. The model for  $N'_{\max}$  deals only with gas phase interactions between the analyte and matrix and not interferences that may affect the vaporization of the analyte. Our earlier simplification, that  $\tau_1$  is constant, causes  $N'_{\max}/N_0$  to remain constant for different values of  $\tau_2/\tau_1$ . In the presence of a chemical interference, a drop in pressure will result in fewer collisions that will reduce the number of A–B dimers formed in the gaseous phase. This may lead to a larger signal at lower pressures or, rather, lower values of  $\tau_2/\tau_1$ . Convolution of this matrix-controlled curve with the vaporization/diffusion curve results in the peak labeled "max" in Figure 1c, which occurs at a lower level of  $\tau_2/\tau_1$  than the peak observed for  $N'_{\max}/N_0$ . This shift in peak maximum suggests that the maximum signal will occur at a lower pressure where matrix interference is minimized and residence time maximized. The

(21) Atkins, P. W. *Physical Chemistry*; W. H. Freeman: New York, 1982.

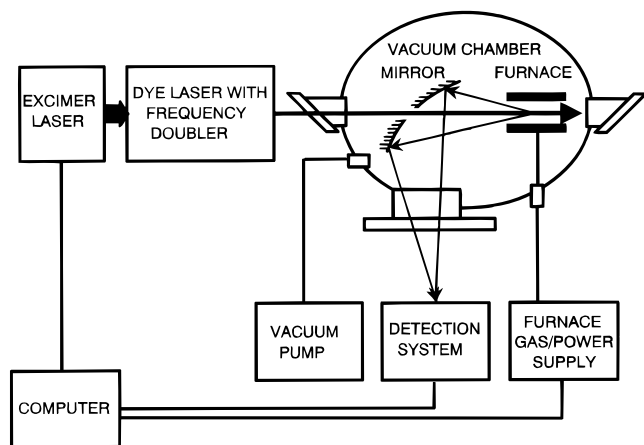


Figure 2. Schematic diagram of the VETA-LEAFS instrumentation.

model cannot predict the exact pressure that corresponds to a maximum signal, hence this maximum can be above or below atmospheric pressure.

From the literature reports<sup>5,19,20</sup> and the above model, optimization of the working pressure may improve graphite furnace analyses for some elements. The above model shows that changes in either the residence time of the analyte or the atomization efficiency can affect analytical sensitivity. The model predicts that gas phase interactions between analyte and matrix may be reduced at lower working pressures due to a shorter residence time for both analyte and matrix. Although the model does not quantitatively predict how reduced working pressures will affect the vaporization of the analyte, literature reports<sup>7-9</sup> have shown that a reduction in working pressure may improve atomization efficiency. Both the model and the suggestion made in the literature<sup>11-13</sup> were tested in the current work. Several SRM samples were analyzed by dissolution and direct analysis, at atmospheric and reduced working pressures. Glass and nickel alloy standard reference materials were chosen for this investigation because they are difficult to atomize completely, and often produce matrix interferences.

## EXPERIMENTAL SECTION

**Instrumentation.** A schematic diagram of the instrumentation is shown in Figure 2. The laser system for ETA-LEAFS has been described previously and is briefly summarized here.<sup>14,22,23</sup> An excimer laser, operated with xenon chloride (308 nm) at a repetition rate of 500 Hz, was used to pump a tunable dye laser equipped with a frequency doubler. The excimer and dye lasers (Lambda Physik, Gottingen, Germany) were Models EMG 104 MSC and FL3002E, respectively. Tellurium, phosphorus, and platinum were excited at 213.618, 212.861, and 214.281 nm, respectively. Cobalt was excited at either 217.460 or 304.400 nm. The optimal frequency-doubled laser energies for excitation were 10  $\mu$ J/pulse for cobalt and platinum and 1  $\mu$ J/pulse for tellurium and phosphorus. The dye required to tune the laser between 206 and 222 nm<sup>24</sup> was stilbene 420 [2,2'-(1,1'-biphenyl)-4,4'-diyl-di-2,1-ethenediyl]bis(benzenesulfonic acid) disodium salt (Exciton,

Dayton, OH)]. Stilbene 420 was dissolved in absolute methanol (Brand-Nu Laboratories, Meriden, CT) to working concentrations of 0.65 and 0.22 g L<sup>-1</sup>, in the oscillator and amplifier dye cells, respectively.  $\beta$ -Barium borate-2 was the frequency-doubling crystal used in conjunction with stilbene 420. The dye required to tune the laser between 294 and 322 nm<sup>24</sup> was rhodamine 610 [*o*-[6-(diethylamino)-3-(diethylimino)-3*H*-xanthe-9-yl]benzoic acid; Exciton). Rhodamine 610 was dissolved in absolute methanol to working concentrations of 0.91 and 0.30 g L<sup>-1</sup> in the oscillator and amplifier dye cells, respectively. KDP was the frequency-doubling crystal used in conjunction with rhodamine 610. For the determination of cobalt in glass, use of the 217/235 nm excitation/detection scheme and stilbene 420 was more convenient. The detection limits (3 $\sigma$ ) for cobalt with excitation/detection schemes of 304/340.5 and 217/235.0 nm were 20 fg and 3.0 pg, respectively.

The atomizer was a Perkin-Elmer HGA-500 graphite furnace (Perkin-Elmer, Norwalk, CT) used with pyrolytically coated graphite furnaces and L'vov platforms. The furnace was enclosed in a laboratory-designed cylindrical vacuum chamber that was constructed from stainless steel. The interior of the chamber had a volume of  $\sim$ 10 L. The pressure in the chamber could be adjusted between atmospheric and 5 Pa. Approximately 1–2 min was required to evacuate the chamber to a final pressure of 5 Pa. The chamber was equipped with a removable lid that was located just above the furnace and allowed for sample input. The windows on the vacuum chamber and on the furnace were angled to reduce stray laser background radiation.<sup>25</sup> Pyrolysis/atomization temperatures were 800/1600  $^{\circ}$ C for tellurium, 800/2600  $^{\circ}$ C for platinum, 1000/2600  $^{\circ}$ C for phosphorus, 1000/2400  $^{\circ}$ C for cobalt with detection at 340.5 nm, and 1000/2600  $^{\circ}$ C for cobalt with detection at 235.0 nm. Argon (The Aero All-Gas Co., Hartford, CT), with no more than 0.001% oxygen and nitrogen, served as the sheath gas. Atomization was conducted in the gas stop mode at a maximum heating rate of 1500  $^{\circ}$ C s<sup>-1</sup>. Calibration of the atomization temperature to  $\pm$ 50  $^{\circ}$ C was achieved by use of an optical pyrometer.

Fluorescence was detected at 180 $^{\circ}$  to the direction of the laser beam, in a scheme called front surface illumination.<sup>26</sup> An off-axis ellipsoidal mirror (Aero Research Associates Inc., Port Washington, NY), with an aluminum reflective surface and a magnesium fluoride overcoat,<sup>27</sup> was used to reflect the fluorescence from the graphite furnace onto the slit of a monochromator (ISA, Model H-10, Metuchen, NJ). For tellurium, platinum, and phosphorus, fluorescence was detected at 238.4, 241.0, and 253.5 nm, respectively. The amount of stray laser radiation that entered the monochromator was minimized through the use of Schott color glass filters (ESCO Products, Oak Ridge, NJ) placed in front of the monochromator entrance slit. A UG-5 filter (transmittance 95% at 253 nm, <0.01% at 213 nm) was used in conjunction with stilbene 420, and a 7-64 filter (transmittance 56% at 340 nm, <0.01% at 304 nm) was used in conjunction with rhodamine 610. The detection system consisted of a 2 in. end-on, high-gain, photomultiplier tube (Thorn-EMI, Model 9893QB-350, Fairfield, NJ), a preamplifier (LeCroy, Model VV100BTB, Spring Valley, NY) with a gain of 10, and a boxcar integrator (PAR, Model 162/165,

(22) Irwin, R. L.; Wei, G.-T.; Butcher, D. J.; Liang, Z.; Su, E. G.; Takahashi, J.; Walton, A. P.; Michel, R. G. *Spectrochim. Acta, Part B* **1992**, *47B*, 1497.

(23) Dougherty, J. P.; Preli, F. R., Jr.; McCaffrey, J. T.; Seltzer, M. D.; Michel, R. G. *Anal. Chem.* **1987**, *59*, 1112–1119.

(24) Brackmann, U. *Lambdachrome Laser Dyes*; Lambda Physik GmbH, Gottingen, West Germany, 1986.

(25) Wei, G.-T.; Dougherty, J. P.; Preli, F. R., Jr.; Michel, R. G. *J. Anal. At. Spectrom.* **1990**, *5*, 249–259.

(26) Goforth, D.; Winefordner, J. D. *Anal. Chem.* **1986**, *58*, 2598–2602.

(27) Yuzefovsky, A. I.; Lonardo, R. F.; Michel, R. G. *Anal. Chem.* **1995**, *67*, 2246–2255.

Princeton, NJ) with a gate width of 50 ns, a gate time constant of 0.5  $\mu$ s, and an output time constant of 1 ms. The integrated signal, peak area, used throughout this work was acquired with a personal computer (Dell PC 200-80286) equipped with Asyst software (Rochester, NY).

**Reagents.** All samples and standards were prepared either in a class 100 (U.S. Federal 209b) clean air hood or on a class 100 clean bench. Subboiled distilled water and ultrapure acids (Baker Inc., Jackson, TN) were used for all standard and sample preparation. All glassware and plasticware were soaked in 20% nitric acid (Reagent grade, Baker Inc.) for 24 h and then rinsed with subboiled distilled water prior to use. A stock solution of 1000 ppm cobalt was prepared by dissolution of cobalt powder (HiPure grade, Spex Industries, Metuchen, NJ) in a minimum volume of (1+1) HCl followed by dilution with 1% (v/v) HCl. A stock solution of 1000 ppm phosphorus was prepared by dissolution of ammonium dihydrogen phosphate (HiPure grade, Spex Industries) in water. A stock solution of 1000 ppm platinum in 10% HCl (HiPure grade) was obtained from Spex Industries. A stock solution of 1000 ppm tellurium was prepared by dissolution of tellurium metal in a minimum volume of concentrated nitric acid. The solution was then diluted to  $\sim$ 50 mL, followed by the addition of a minimum volume of concentrated HCl to redissolve the precipitate. The solution was then gently heated to  $\sim$ 60  $^{\circ}$ C to expel oxides of nitrogen, cooled, and then diluted to 1 L. Stock solutions were diluted with 0.2% nitric acid to generate working standards. A 0.2% solution of nitric acid served as the blank for all analytes.

**Sample Preparation.** The following quantitative determinations were made in SRM obtained from the National Institute of Standards and Technology (NIST, Gaithersburg, MD): phosphorus in nickel alloys, SRM 349, 865, 1208-1, and 126c; tellurium in nickel alloys, SRM 897; and cobalt in glass, SRM 613. For the dissolution of nickel alloys,  $\sim$ 100 mg of each alloy was weighed into a poly(tetrafluoroethylene) (PTFE) beaker, to which was added 2 mL of water, hydrochloric acid, and nitric acid and 0.5 mL of hydrofluoric acid. These solutions were then heated at  $\sim$ 60  $^{\circ}$ C for 20 min to ensure complete dissolution before dilution to 100 mL. For the dissolution of glass,  $\sim$ 100 mg of pulverized glass was weighed into a PTFE beaker, to which was added 8 mL of hydrofluoric acid, 3 mL of perchloric acid, and 3 mL of nitric acid. Solutions were heated at  $\sim$ 80  $^{\circ}$ C for several hours periodically over the course of 4–5 days to ensure complete dissolution followed by dilution to 100.0 mL in polyethylene volumetric flasks. The addition of two 2 mL portions of hydrofluoric acid during the dissolution was necessary to compensate for evaporation of hydrofluoric acid. For both dissolution methods, sample blanks were prepared in an identical manner.

**Analytical Procedures.** Quantitative results were based on the measurement of temporal peak areas produced from 20  $\mu$ L aliquots of standard or sample solutions followed by subtraction of a blank. Direct solid sample analysis was performed by introduction of a solid chip, with a weight between 0.1 and 2.0 mg, directly onto the L'vov platform. For direct solid analysis, the peak areas produced by  $\sim$ 10 separate chips were normalized as a function of the individual sample masses. Solid sampling was conducted without a dry or char step, and calibration was achieved with aqueous standards. During the construction of calibration graphs, attenuation of the signal radiation was necessary to ensure a linear response from the photomultiplier tube.

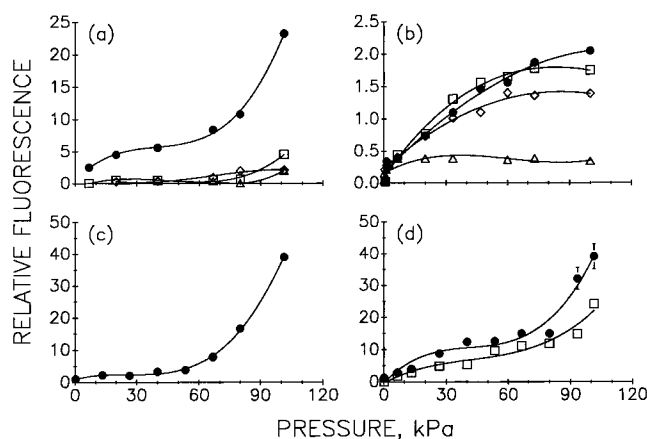


Figure 3. Effect of pressure on the relative fluorescence signals produced from the following: (a) 20 ng of aqueous phosphorus with 20  $\mu$ g of aqueous nickel modifier, atomization temperatures ( $\bullet$ ) 2600, ( $\square$ ) 2400, and ( $\diamond$ ) 2200  $^{\circ}$ C; and ( $\triangle$ ) 200 ng of aqueous phosphorus without nickel, atomization temperature 2600  $^{\circ}$ C. (b) 200 pg of aqueous cobalt, atomization temperatures ( $\bullet$ ) 2400, ( $\square$ ) 2200, ( $\diamond$ ) 2000, and ( $\triangle$ ) 1800  $^{\circ}$ C. (c) Cobalt in SRM 613, 0.1023 g/100 mL (3.63  $\mu$ g of cobalt) atomization temperature 2600  $^{\circ}$ C, Ex/FI 217.460/235.0 nm. (d) 10 ng of aqueous platinum, atomization temperatures ( $\bullet$ ) 2650 and ( $\square$ ) 2500  $^{\circ}$ C.

Attenuation was achieved by calibrated neutral density filters (ESCO Products) placed directly in front of the entrance slit of the monochromator. Detection limits were obtained by extrapolation of the calibration graphs to a signal level equal to three times the blank noise, which was the standard deviation of 16 measurements of the blank.

## RESULTS AND DISCUSSION

**Effect of Reduced Pressure on Analytical Sensitivity for Phosphorus in Nickel Matrices.** In solution, nickel has been shown to be a chemical modifier to facilitate the vaporization of phosphorus, but phosphorus cannot be vaporized from a solid nickel matrix, at atmospheric pressure, due to its low volatility.<sup>16</sup> Low-pressure vaporization was tested here in an attempt to increase the atomization efficiency of phosphorus in the presence of nickel. Plots of relative fluorescence versus working pressure were obtained for 20 ng of aqueous phosphorus with 20  $\mu$ g of aqueous nickel modifier at atomization temperatures of 2600, 2400, and 2200  $^{\circ}$ C and 200 ng of aqueous phosphorus without nickel at an atomization temperature of 2600  $^{\circ}$ C. The results are shown in Figure 3a. The only appreciable sensitivity for phosphorus was obtained with an atomization temperature of 2600  $^{\circ}$ C and nickel modification. Analytical sensitivity was found to decrease rapidly as the pressure was lowered from atmospheric pressure to 70 kPa and to decrease more slowly as the pressure was further lowered to 7 kPa. The reduced sensitivity at lower working pressures suggested that there was no increase in the vaporization of aqueous phosphorus, and the decrease in recovery was primarily due to increased analyte diffusion. Wang and Holcombe<sup>8</sup> observed the same effect for vanadium for ETA-AAS and noted that if increased diffusion were solely responsible for the decrease in signal at lower pressures, a linear relationship should be obtained between pressure and signal. They postulated that the nonlinearity may have resulted from a combination of an increase in diffusion with an increase in the relative absorbance due to a narrowing of the absorbance spectral profile.

Phosphorus was measured in SRM nickel-based alloys 349, 865, 1208-1, and 126c by ETA-LEAFS<sup>16</sup> with dissolution and solid

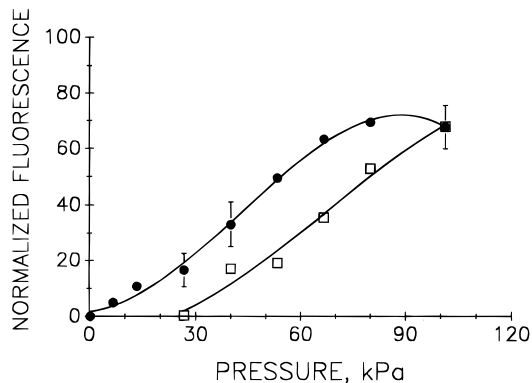


Figure 4. Effect of pressure on the normalized fluorescence signals produced from (●) tellurium in SRM 897 (1.05  $\mu\text{g}$  of tellurium/g of alloy) (each point represents the average and standard deviation of the peak areas produced from 10 solid chips normalized by sample mass) and (□) 160 pg of aqueous tellurium.

sampling and by VETA-LEAFS with direct solid analysis. Dissolution of the alloys followed by analysis at atmospheric pressure produced quantitative results that were in agreement with certified values at the 95% confidence level. In the case of solid sampling at atmospheric pressure, less than 5% of the phosphorus contained in the nickel alloy could be vaporized. For the VETA-LEAFS method, ~2% of the analyte was recovered at a pressure of 80 kPa, and essentially no recovery was obtained at pressures lower than 80 kPa. Hence, reduced working pressure failed to increase the atomization efficiency for phosphorus, atomized from either an aqueous solution or a nickel matrix.

**Effect of Reduced Pressure on Analytical Sensitivity for Tellurium in Nickel Matrices.** Unlike phosphorus, tellurium is relatively volatile and can be vaporized from a solid nickel matrix at atmospheric pressure with an atomization temperature of 1800 °C.<sup>17</sup> Previously, aqueous calibration conducted at atmospheric pressure was successful for tellurium atomized either from a solution of dissolved alloy or directly from a nickel alloy.<sup>17</sup> As shown in Figure 4, the effects of low-pressure vaporization were investigated through plots of normalized fluorescence versus working pressure for both a standard solution of tellurium and tellurium contained in SRM 897. Analytical sensitivity decreased by ~1 order of magnitude as the pressure was decreased from atmospheric pressure to 7 Pa. Reduction in working pressure was more detrimental to the analytical sensitivity obtained for aqueous tellurium than tellurium atomized directly from the solid. Matrix modification may allow for aqueous calibration under reduced pressure, but this possibility was not investigated since calibration was already possible at atmospheric pressure, where the sensitivities were the same. For tellurium atomized directly from the solid alloy, no change in sensitivity was observed as the working pressures was reduced from atmospheric pressure to ~70 kPa. If a reduction in working pressure affected only the residence time of the analyte, poorer sensitivity should have been obtained. According to the above theoretical model, only increased vaporization of the tellurium from the solid matrix could account for the maintenance of the sensitivity at a lower working pressure. If this is true, low-pressure vaporization would be advantageous in cases where matrix interferences are present because gas phase interactions between analyte and matrix may be minimized without a loss in sensitivity.

**Effect of Reduced Pressure on Analytical Sensitivity for Cobalt in Quartz Glass.** Bolshov et al.<sup>11–13</sup> employed VETA-

LEAFS without STPF technology for the direct determination of cobalt in quartz glass. The matrix was removed via a char step under vacuum as discussed earlier. We attempted to reproduce their work, but with STPF conditions. A preliminary step was to determine the effect of pressure on the analytical sensitivity of cobalt with different atomization temperatures. The results are shown in Figure 3b. With an atomization temperature of 2400 °C, the sensitivity decreased by ~1 order of magnitude as the working pressure was decreased from atmospheric pressure to 250 Pa. Lower atomization temperatures were used to delay the rate of analyte supply into the furnace in order to increase the total residence time of analyte, and thus improve the sensitivity. With atomization temperatures of 2200 and 2000 °C, the working pressure could be reduced to 40 kPa without a significant decrease in sensitivity. These results are similar to those obtained for tellurium. Atomization conducted at this reduced pressure may be used to minimize matrix effects in the gas phase at the cost of a slight decrease in sensitivity. The use of 1800 °C as the atomization temperature resulted in poor sensitivity, which did not change as a function of working pressure, due to incomplete atomization.

To reproduce the work done by Bolshov et al.,<sup>11–13</sup> the effect of working pressure on the sensitivity for cobalt in glass (SRM 613) atomized directly from the solid, and from a solution of dissolved glass, was investigated. Only 0.1% of the cobalt could be directly atomized from the glass matrix at atmospheric pressure, and essentially no recovery was observed with lower working pressures. Atomization of cobalt from a solution of dissolved glass was possible, and the effect of working pressure on the analytical sensitivity is shown in Figure 3c. A reduction in working pressure from atmospheric to 7 Pa resulted in a decrease in sensitivity by 2 orders of magnitude. Hence, low-pressure vaporization did not improve the atomization efficiency for cobalt atomized from either the glass matrix or the aqueous solution. The only result was a lower sensitivity at reduced pressures due to increased diffusion of the analyte.

The plateau in Figure 3b that corresponds to cobalt atomized at 1800 °C is similar to those observed by Donega and Burgess.<sup>7</sup> As mentioned previously, they investigated the effect of foreign gas pressure on the absorption signals for aluminum and sodium by ETA-AAS with boat atomization. No change in sensitivity was observed as the working pressure was decreased from 40 to 13 kPa, and a decrease in sensitivity as the pressure was decreased further. No data were reported for pressures greater than 40 kPa. The constant sensitivity in the pressure region of 13–40 kPa may have resulted from incomplete atomization associated with their non-STPF technique.

In the current work, quartz glass was analyzed for the determination of cobalt by ETA-LEAFS with both dissolution and direct solid analysis, and by VETA-LEAFS with direct solid analysis. The glass investigated was SRM 613, which has an uncertified value of 35.5 ppm. For the determination of cobalt in glass by ETA-LEAFS with dissolution followed by aqueous calibration, an experimental value of  $32.5 \pm 2.0$  ppm was obtained. Direct solid analysis, conducted both at atmospheric pressure and at 80 kPa, was unsuccessful because only 0.1% of the analyte could be vaporized. No recovery was observed for samples atomized below 80 kPa. Thus, similar to phosphorus, low-pressure vaporization was not beneficial.

**Determination of Platinum by VETA-LEAFS and the Effect of Pressure on Signal Profiles.** Platinum is considered to be an involatile element in a graphite furnace.<sup>28</sup> Brown and Lee<sup>28</sup> investigated the peak profiles and appearance times for several involatile and refractory elements atomized at atmospheric pressure in furnaces composed entirely of pyrolytic graphite. They employed a Philips analytical graphite furnace system (Model PU9095) that was heated to a maximum temperature of 2800 °C. The elements studied were platinum, vanadium, molybdenum, and titanium. Temporal signal profiles were unsymmetrical due to peak tailing. In the case of vanadium, molybdenum, and titanium, complete atomization was not possible.

The maximum atomization temperature that is attainable by our Perkin-Elmer graphite furnace system<sup>2</sup> is 2650 °C. At this temperature, temporal signals obtained for platinum at atmospheric pressure are typically unsymmetrical due to incomplete atomization. VETA-LEAFS was applied in an attempt to improve both the atomization efficiency and the temporal profiles. Figure 3d shows the effect of working pressure on the analytical sensitivity for 10 ng of platinum atomized at 2650 and 2500 °C. For atomization at 2650 °C, the sensitivity decreased rapidly as the working pressure was lowered from atmospheric pressure to 70 kPa and then decreased more slowly as the pressure was lowered to 7 Pa. For atomization at 2500 °C, reduction in working pressure had a similar effect on analytical sensitivity. These results were analogous to those obtained for the other elements investigated.

Although VETA-LEAFS failed to improve the atomization efficiency, a reduction in peak tailing was observed in the temporal profiles. Panels a and b of Figure 5 show the temporal signal profiles for 0.10 pg of platinum atomized at atmospheric pressure and 1.0 pg of platinum atomized at 7 Pa, respectively. A working pressure of 7 Pa was sufficient to minimize peak tailing, but 10 times as much platinum was required to produce a peak with approximately the same peak height. An improvement in temporal resolution would be beneficial for situations in which there is an overlap between two or more unresolved peaks due to different chemical species, although overlaps of this nature are extremely rare in ETA-LEAFS and ETA-AAS.

## CONCLUSIONS

The essence of STPF technology, for atomic spectrometry in graphite furnaces, is complete atomization of the analyte with a minimum of chemical and physical interferences. In some cases, complete atomization of the analyte is not possible due to the involatility of the analyte, matrix, or both. Here, low-pressure vaporization was combined with STPF technology in an attempt to improve these situations. The model developed in this work predicted that the atomization efficiency of an analyte can be maximized through optimization of the working pressure. At this optimal pressure, gas phase interactions between the analyte and

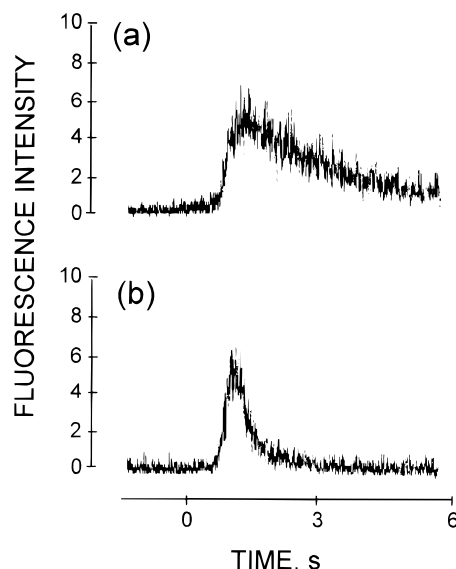


Figure 5. Signal profiles for aqueous platinum: (a) 0.10 pg, atmospheric pressure; (b) 1.0 pg, working pressure 7 kPa.

matrix would be minimized, and analyte residence time would be maximized. The model was unable to predict whether this pressure would be below or above atmospheric pressure. The ability to directly atomize tellurium and cobalt at a somewhat reduced pressures, without significant changes in sensitivity, suggested that any decrease in sensitivity due to diffusion of the analyte was compensated by a commensurate increase in the vaporization of the analyte. These results are in direct agreement with the theoretical model developed here. Atmospheric pressure seems to be close to the optimal working pressure since small changes in working pressure, below atmospheric pressure, did not produce large changes in sensitivity. Finally, working pressures lower than 1 atm may be useful in instances where a shift in the linear dynamic range, or better temporal resolution, is required.

## ACKNOWLEDGMENT

Some of the equipment used in this work was purchased with funds from The National Institute of Health Grant GM 32002. The authors are indebted to John E. Gammerino of The University of Connecticut, who provided valuable insight during the construction of the vacuum chamber used in this work. Presented in part at the XX Annual FACSS Conference, Detroit, MI, October 1993, at the 45th Pittsburgh Conference, Chicago, IL, February 1994, and at the 33rd Eastern Analytical Symposium and Exposition, Somerset, NJ, November 1994.

Received for review September 6, 1995. Accepted November 13, 1995.\*

AC9509014

(28) Brown, A. A.; Lee, M. *Fresenius' J. Anal. Chem.* **1986**, 323, 697–702.

\* Abstract published in *Advance ACS Abstracts*, January 1, 1996.